Inorg. Chem. **2009**, *48*, 1053−1061

Strategy for the Stereochemical Assignment of Tris-Heteroleptic Ru(II) Complexes by NMR Spectroscopy

Xiulan Xie,* Seann P. Mulcahy, and Eric Meggers

Philipps-Universität Marburg, Hans-Meerwein-Straβe, 35043 Marburg, Germany

Received September 10, 2008

The relative stereochemistry of tris-heteroleptic ruthenium complexes $[Ru(pp)(pp')(pp'')](PF_6)_2$, where pp = 1,10-phenanthroline-4-carboxamide, pp′ = 5,6-dimethyl-1,10-phenanthroline, and pp″ = 7,8-dimethyl dipyrido[3,2-a:2′,3′-c]phenazine, was studied using NMR spectroscopy. The ^1H and ^{13}C spectra were assigned by using double-quantum-filtered correlation spectroscopy (DQF-COSY), heteronuclear single-quantum correlation (HSQC), and heteronuclear multiple-bond correlation (HMBC) experiments for the two diastereomers, each a pair of enantiomers. Nuclear Overhauser effect contacts between the neighboring ligands differentiated the two halves of each symmetrical ligand, thus enabling a full assignment of the NMR signals and an accurate determination of the relative stereochemistry of the complexes. The introduction of an additional chiral center to ligand pp by coupling it with L-lysine caused removal of the enantiomerism. Thus, four diastereomers were observed and their relative stereochemistry determined.

Introduction

Ruthenium(II) polypyridyl complexes are of great interest due to their unique photochemical, photophysical, and electrochemical properties.[1] Significant precedent exists for the development of synthetic routes for the preparation of $[Ru(pp)(pp')(pp'')]Cl_2$ complexes.[2−10] Very recently, we developed a convenient solid-phase synthetic route to produce structurally unique tris-heteroleptic ruthenium(II) polypyridyl complexes in high purity and good yields.[11] These complexes have been developed as acetylcholinesterase inhibitors,[12] and in the course of our studies, we recognized that stereochemical assignment of the most active isomer posed a significant challenge. Here, we present our method for the full characterization of the relative stereochemistry as determined by NMR spectroscopy. A schematic view of the complexes used in this study is given in Figure 1. The ligands for complex **1** are pp = 1,10-phenanthroline-4-carboxamide, pp′ = 5,6-dimethyl-1,10-phenanthroline (Me_2phen), and pp″ = 7,8-dimethyl dipyrido[3,2-a:2′,3′-c]phenazine (dppz), whereby pp′ and pp″ have C_{2v} and pp has C_1 symmetry. An octahedral arrangement of these ligands around the metal center results in four different structures: two pairs of racemic diastereomers. We have succeeded in separating the two diastereomers, which differ only in the orientation of pp, and assigned the two complexes to be diastereomers **a** and **b**. Sketches of the diastereomers of complex **1** are presented in Figure 1 as the Δ-enantiomers **Δ−1a** and **Δ−1b**, while the corresponding racemic ones will be referred to as **rac−1a** and **rac−1b**, respectively. By attaching L-lysine to the pp ligand, we introduced an additional chiral center and obtained four different stereoisomers, complexes **Δ−2a**, **Δ−2b**, **Λ−2a**, and **Λ−2b**, as shown in Figure 1. In this paper, we present our NMR studies and the assignment of these diastereomers.

* Author to whom correspondence should be addressed. E-mail: xie@staff.uni-marburg.de.

(1) Juris, A.; Balzani, V.; Barigelletti, F.; Campagna, S.; Belser, P.; von Zelewsky, A. *Coord. Chem. Rev.* **1988**, *84*, 85–277.
(2) Krause, R. A. *Inorg. Chim. Acta* **1977**, *22*, 209–213.
(3) Black, D. S. C.; Deacon, G. B.; Thomas, N. C. *Inorg. Chim. Acta* **1982**, *65*, L75−L76.
(4) Thummel, R. P.; Lefoulon, F.; Chirayil, S. *Inorg. Chem.* **1987**, *26*, 3072–3074.
(5) von Zelewsky, A.; Gremaus, G. *Helv. Chim. Acta* **1988**, *71*, 1108–1115.
(6) Strouse, G. F.; Anderson, P. A.; Schoonover, I. R.; Meyer, T. J.; Keene, F. R. *Inorg. Chem.* **1992**, *31*, 3004–3006.
(7) Anderson, P. A.; Deacon, G. B.; Haarmann, K. H.; Keene, F. R.; Meyer, T. J.; Reitsma, D. A.; Skelton, B. W.; Strouse, G. F.; Thomas, N. C.; Treadway, J. A.; White, A. H. *Inorg. Chem.* **1995**, *34*, 6145–6157.
(8) Zakeeruddin, S. M.; Nazeerudin, M. K.; Humphry-Baker, R.; Grätzel, M. *Inorg. Chem.* **1998**, *37*, 5251–5259.
(9) Freedman, D. A.; Evju, J. K.; Pomije, M. K.; Mann, K. R. *Inorg. Chem.* **2001**, *40*, 5711–5715.
(10) Mulhern, D.; Brooker, S.; Gorls, H.; Rau, S.; Vos, J. G. *Dalton Trans.* **2006**, 51–57.

10.1021/ic801744a CCC: $40.75
Published on Web 12/23/2008

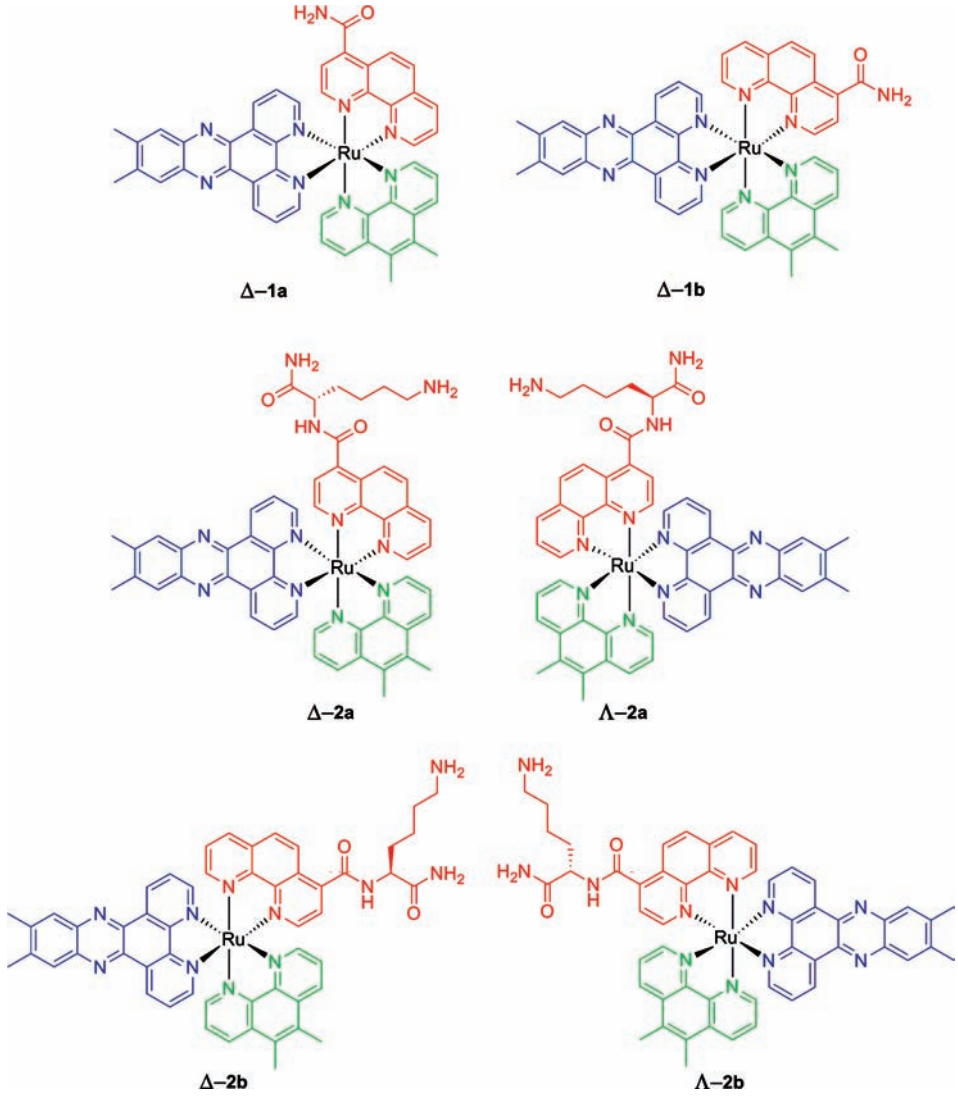

Figure 1. Sketches of the diastereomers of complex **1** in Δ form and all the diastereomers of complex **2**.

To our knowledge, there are relatively few published articles dealing with the NMR spectroscopic characterization of tris-heteroleptic ruthenium complexes, often due to the complexity of the NMR spectra of such complexes. Mulhern et al. described the crystal structure of [Ru(bpy)(Me_2bpy)(bpt)]Cl (bpy = 2,2′- bipyridine, Me_2bpy = 4,4′-dimethyl-2,2′-bipyridine, Hbpt = 3,5-bis(pyridin-2-yl)-1,2,4-triazole) and noticed stereoisomerism due to the appearance of more than one set of methyl resonance signals in the ^{1}H spectrum.[10] Freedman et al. presented a thorough characterization of [Ru(bpy)(Me_2bpy)(phen)]Cl_2 (phen = 1,10-phenanthroline) by using correlation spectroscopy (COSY).[9] A full signal assignment was performed on the basis of an assumption of different ring current anisotropy in the bpy and phen ligands. Additionally, Anderson et al. reported the crystal structure of $[Ru(Me_2bpy)(phen)(bpa)]^{2+}$ (bpa = bis(2-pyridyl)amine), whereby all three ligands are symmetric.[7] However, it was noticed that the two halves of each ligand are in magnetically inequivalent environments and therefore show a difference in ^{1}H chemical shift. Finally, Orellana et al. carried out studies on a series of tris-homoleptic Ru(II) complexes and documented the coordination-induced shifts in ^{1}H and ^{13}C signals.[13] Here, we present a thorough characterization of the complex structure of **1** by using two-dimensional homonuclear NMR, as well as heteronuclear ^{1}H−^{13}C correlation measurements. Further, nuclear Overhauser effect spectrometry (NOESY) were used to assign the two halves of each symmetrical ligand, leading to an assignment of the relative stereochemistry.

Materials and Methods

General Procedures. All solid-supported reactions were shaken orbitally in test tubes under an inert nitrogen atmosphere. SynPhase L-Series Polystyrene (MIL1033) lanterns were purchased from Mimotopes Pty Ltd. (Clayton Victoria, Australia) and kept at 4 °C before use. The peptide coupling reagent (benzotriazol-1-yloxy) tripyrrolidinophosphonium hexafluorophosphate (PyBOP) and Fmoc-Lys(Boc)-OH were obtained from Fluka and stored at +4 and −20 °C, respectively. Anhydrous

(11) Mulcahy, S. P.; Li, S.; Korn, R.; Xie, X.; Meggers, E. *Inorg. Chem.* **2008**, *47*, 5030–5032.
(12) Dwyer, F. P.; Gyarfas, E. C.; Rogers, W. P.; Koch, J. H. *Nature* **1952**, *170*, 190–191.
(13) Orellana, G.; Ibarra, C. A.; Santoro, J. *Inorg. Chem.* **1988**, *27*, 1025–1030.

DMF was obtained from Aldrich and further dried over molecular sieves (4 Å, 8−12 mesh). EtOH was obtained from Fisher and dried over molecular sieves. All other solvents (including wash DMF) were HPLC-grade-quality obtained from Fisher unless otherwise noted. All other reagents were obtained from Acros, Aldrich, or Alfa Aesar and used without further purification. A mixture of $[Ru(Me_2phen)(CH_3CN)_3Cl]Cl$ and $[Ru(Me_2phen)(CH_3CN)_2Cl_2]$, 1,10-phenanthroline-4-carboxylic acid, and 7,8-dimethyl dipyrido[3,2-a:2′,3′-c]phenazine were synthesized according to previously reported methods.[11] High-resolution mass spectra were obtained on a Thermo Finnigan LTQ FT instrument using ES ionization. Infrared spectra were recorded on a Nicolet 510 M FT-IR spectrometer. Separation of stereoisomers was performed on an Agilent 1200 Series HPLC System with fraction collection. Molecular modeling was performed using the program CaChe (Fujitsu) using energy minimization.

Synthesis of 1. A total of 15 polystyrene lanterns were swollen in CH_2Cl_2 overnight and washed with CH_2Cl_2. The lanterns were then Fmoc-deprotected with 30 mL of 20% piperidine/DMF with shaking for 45 min. After washing with CH_2Cl_2, MeOH, and DMF extensively, the lanterns were treated with 4-CO_2H-phenanthroline (152 mg, 0.68 mmol), PyBOP (364 mg, 0.68 mmol), and DIPEA (118 μL, 0.68 mmol) in 6.75 mL of dry DMF, and the tube was shaken at 80 °C for 4 h. After extensive washing as described above, the lanterns were subjected to similar conditions: treatment with 4-CO_2H-phenanthroline (100 mg, 0.45 mmol), PyBOP (243 mg, 0.45 mmol), and DIPEA (39 μL, 0.45 mmol) in 2.23 mL of dry DMF and shaking for 2 h at 78 °C. After extensive washing, a capping procedure was performed with 34.5 mL of 8:1:1 DMF/Ac_2O/DIPEA with shaking for 45 min. The lanterns were washed and suspended in dry DMF (6.3 mL) and treated with a mixture of $[Ru(Me_2phen)(CH_3CN)_3Cl]Cl$ and $[Ru(Me_2phen)(CH_3CN)_2Cl_2]$ (226 mg, 0.45 mmol) and heated to 80 °C for 3 h. The lanterns were washed briefly and then retreated with a ruthenium precursor under similar conditions: 113 mg of a mixture of $[Ru(Me_2phen)(CH_3CN)_3Cl]$-Cl and $[Ru(Me_2phen)(CH_3CN)_2Cl_2]$ in 6.3 mL of DMF. Finally, the lanterns were washed and then treated in dry EtOH (38 mL) with 7,8-dimethyl dipyrido[3,2-a:2′,3′-c]phenazine (698 mg, 2.25 mmol) and shaken at 78 °C for 16 h. The lanterns were washed extensively, and then the metal complex was removed from the resin in 10 mL of 95% aqueous TFA with shaking for 4 h. The lanterns were washed, and the filtrate was concentrated to give a red-orange residue. The crude material was purified by silica gel column chromatography using a mobile phase gradient from 100:3:1 to 50:6:2 MeCN/H_2O/KNO_3 (saturated aqueous). The product was redissolved in minimal EtOH/H_2O (∼1:2) and precipitated with saturated aqueous NH_4PF_6, filtered, and washed with H_2O to give **1** (25 mg, 10%) as an orange solid. HPLC separation of the two diastereomers of **1** was achieved on an analytical reverse phase column (Merck PuroSphere Star RP-8e, 250 mm × 4.6 mm, 5 μm). The compound was dissolved in MeCN or MeCN/H_2O mixtures and passed through a 2 μm filter. The sample was then eluted on a 5 μm Merck LiChroCART 250-4 Purospher STAR RP-8 endcapped column. The mobile phase consisted of 0.1% aqueous TFA and MeCN. Isocratic elutions at 37% MeCN were performed at a pressure of 115 bar, a flow rate of 1 mL/min, a temperature of 50 °C, and a detection wavelength of 254 nm. Analytical data for ^{1}H NMR (DMSO-d_6): see the Supporting Information. ^{13}C NMR (DMSO-d_6): see the Supporting Information. IR (thin film) N (cm^{-1}): 3308, 3087, 2927, 2857, 1769, 1684, 1472, 1427, 1409, 1377, 1357, 1296, 1201, 1130, 1037, 866, 842, 800, 722. HRMS (ESI) calcd for $RuC_{47}H_{35}N_9OPF_6$: $(M - PF_6)^+$ 988.1644. Found: $(M - PF_6)^+$ 988.1640.

Synthesis of 2. Six polystyrene lanterns were swollen in CH_2Cl_2 for 1 h and washed with CH_2Cl_2. The lanterns were then Fmoc-deprotected with 12 mL of 20% piperidine/DMF with shaking for 45 min. After washing with CH_2Cl_2, MeOH, and DMF extensively, the lanterns were arrayed in a 96-well plate, and 500 μL of a nitrogen-purged solution of Fmoc−Lys(Boc)−OH (365 mg, 0.78 mmol), PyBOP (405 mg, 0.78 mmol), and DIPEA (130 μL, 0.78 mmol) in 3 mL of dry DMF was added on top. The plate was then shaken at room temperature for 4.5 h and the lanterns decanted and washed as before. The lanterns were briefly capped by pooling the lanterns and shaking them in a solution of 14.4 mL DMF/Ac_2O/DIPEA (8:1:1) for 45 min at room temperature. After extensive washing, the lanterns were again Fmoc-deprotected with 12 mL of 20% piperidine/DMF for 45 min, then washed as before and resuspended in 3.15 mL of dry DMF. To this was added 4-CO_2H-phenanthroline (61 mg, 0.27 mmol), PyBOP (145 mg, 0.27 mmol), and DIPEA (47 mL, 0.27 mmol), and the tube was shaken at 70 °C for 4 h. After extensive washing, a capping procedure was performed as described, and the lanterns were stored in CH_2Cl_2 overnight. The next day, the lanterns were washed and suspended in dry DMF (2.5 mL) and treated with a mixture of $[Ru(Me_2phen)(CH_3CN)_3Cl]Cl$ and $[Ru(Me_2phen)(CH_3CN)_2Cl_2]$ (90 mg, 0.18 mmol) and heated to 80 °C for 3 h. The lanterns were washed briefly and then retreated with a ruthenium precursor under similar conditions: 45 mg of a mixture of $[Ru(Me_2phen)(CH_3CN)_3Cl]$-Cl and $[Ru(Me_2phen)(CH_3CN)_2Cl_2]$ in 2.5 mL of DMF. Finally, the lanterns were washed and then treated in dry EtOH (12 mL) with 7,8-dimethyl dipyrido[3,2-a:2′,3′-c]phenazine (136 mg, 0.43 mmol) and shaken at 78 °C for 16 h. The lanterns were washed extensively, and then the metal complex was removed from the resin in 2.4 mL of 95% aqueous TFA with shaking for 4 h. The lanterns were washed, and the filtrate was concentrated to give a red-orange residue. Column chromatography was performed on silica gel from 100% MeCN to 50:6:2 MeCN/H_2O/KNO_3 (sat. aq.). The product was redissolved in 8 mL of EtOH/H_2O (∼1:1) and precipitated with 4 mL of saturated aqueous NH_4PF_6, filtered, and washed with H_2O to give **2** (36 mg, 31%) as an orange solid. HPLC separation of the diastereomeric mixture was performed similarly (isocratic elution at 35% MeCN, 118 bar) as described for **1** to give 16 mg of **rac−2a** and 15 mg of **rac−2b**. Analytical data for ^{1}H NMR (DMSO-d_6): see the Supporting Information. ^{13}C NMR (DMSO-d_6): see the Supporting Information. IR (thin film) N (cm^{-1}): 3406, 3484, 2955, 2927, 2873, 1679, 1541, 1428, 1386, 1335, 1203, 1180, 1133, 866, 839, 801, 722. HRMS (ESI) calcd for $RuC_{55}H_{47}N_{11}O_4F_3$: $(M - TFA)^+$ 1084.2803. Found: $(M - TFA)^+$ 1804.2799.

NMR Measurements. A total of about 7 mg of each sample was dissolved in 0.7 mL of DMSO-d_6. Spectra were recorded at room temperature on a Bruker Avance 600 MHz spectrometer equipped with a 5 mm inverse probe with a z gradient. Double-quantum-filtered correlation spectroscopy (DQF-COSY) and NOESY experiments were performed in the phase-sensitive mode using States-TPPI. NOESY spectra were taken at mixing times of 1.0−2.5 s. Spectra were collected with 16 transients, 4096 points in the F_2 dimension, and 512 increments in the F_1 dimension. NOESY spectra with extra fine resolution in both dimensions were recorded with a spectral width of 2.6 ppm, covering just signals in the aromatic region. A phase-sensitive gradient-selected heteronuclear single-quantum correlation (HSQC) experiment was performed with sensitivity enhancement.[14] Spectra were recorded with 16 transients, 2048 points in the F_2 dimension, and 512 increments in the F_1 dimension, with a spectral width of 12 ppm in the ^{1}H dimension and 180 ppm in the ^{13}C dimension. A gradient-selected hetero-

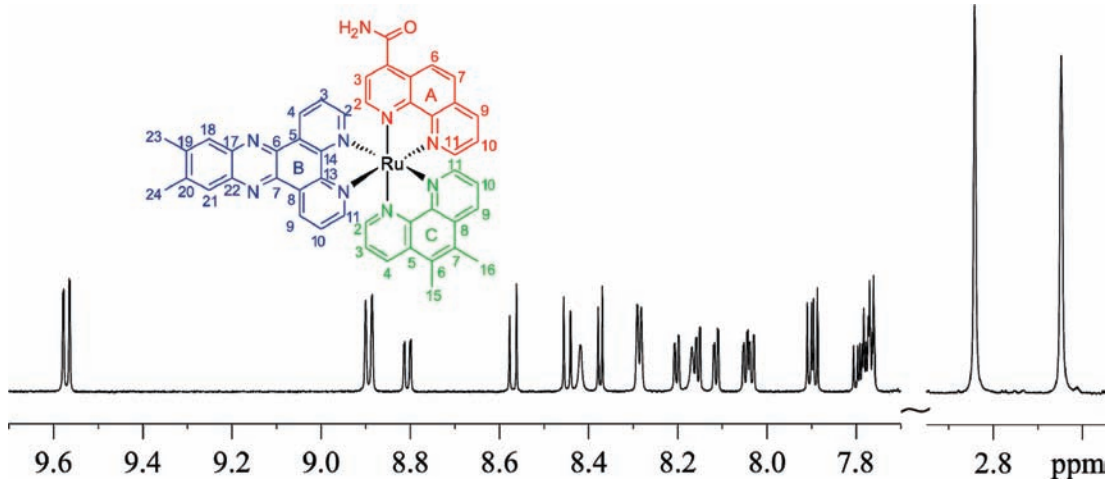

Figure 2. ^{1}H spectrum of **rac−1a**. Sketch of **Δ−1a** with numberings is shown for reference.

nuclear multiple-bond correlation (HMBC) experiment[15] was optimized for coupling of 8 Hz, without decoupling on ^{13}C during acquisition. Spectra were taken with 16 transients, 2048 points in the F_2 dimension, and 256 increments in the F_1 dimension, with a spectral width of 12 ppm in the ^{1}H dimension and 80 ppm in the ^{13}C dimension (covering just the aromatic and the carbonyl signals). In order to have a reliable integral ratio, ^{1}H spectra were acquired with 65 536 data points, 32 transients, and a relaxation delay of 20 s. The ^{13}C spectra were recorded with a Bruker 5 mm BBO probe on a DRX-400 spectrometer. A relaxation delay of 7.5 s was used, and transients between 8000 and 12 000 were recorded. Chemical shifts were referenced to the solvent signal. All spectra were processed with Bruker TOPSPIN 2.1.

Results and Discussion

Resonance Assignments. The ^{1}H spectrum of complex **rac−1a** is shown in Figure 2 together with the ligand assignments and a numbering scheme. The two singlets, each for six protons, at δ 2.65 and 2.84 ppm were observed in the aliphatic region. The former is assigned to the methyl groups B23/24, while the latter is assigned to C15/16, since a COSY cross peak exists between B23/24 and two singlets appearing very close to each other in the aromatic region at δ 8.28 and 8.29 ppm. These two peaks are thus assigned to B18/21 (data not shown). Figure 3 shows a section of the DQF-COSY spectrum of **rac−1a** in the aromatic region. All together, five spin systems were identified: A_1, A_2, A_3, B, and C, with both B and C involving two partially overlapped three-spin systems. For spin system B, a doublet of doublets (dd) for 2H at 7.90 ppm shows cross peaks with a doublet of 2H at 9.57 ppm, and two doublets each of 1H at 8.15 and 8.11 ppm, respectively. The dd was thus assigned to positions 3/10 and the single doublet at 9.57 ppm to positions 4/9, while the two doublets at 8.15 and 8.11 ppm were assigned to positions 2 and 11, respectively. A similar pattern can be seen for spin system C. Spin systems B and C involve structural symmetry and were assigned to ligands B and C.

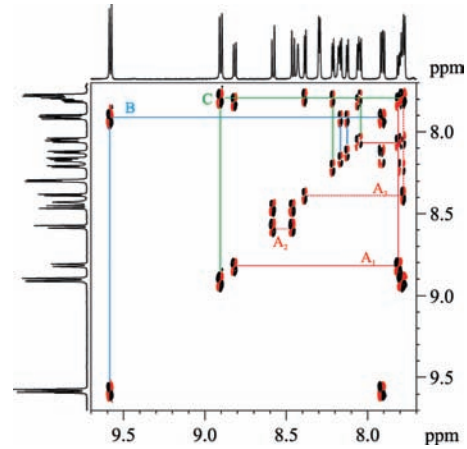

Figure 3. Section of DQF-COSY spectrum of **rac−1a** in the aromatic region. Labels are for the identified spin systems. See text for more details.

Spin system A1 involves three spins, in which a dd of 1H at 7.79 ppm has correlations with the two doublets each of 1H at 8.82 and 8.05 ppm, respectively. Since the proton A10 couples with both protons A9 and A11, the peak at 7.79 ppm was assigned to A10. The distinction between protons A9 and A11 was fulfilled by examining the ^{1}H−^{13}C cross peak of A11 at 8.05−152.83 ppm, which appears in the lower right-hand corner of the HSQC spectrum shown in Figure 4. The peak at 8.05 ppm was thus assigned to the proton A11, and the one at 8.82 ppm to A9. The spin systems A_2 (COSY cross peak 8.57−8.45 ppm) and A_3 (COSY cross peak 8.37−7.77 ppm) each involve just two spins and thus correspond to protons A2−A3 and A6−A7. The observation of the ^{1}H and ^{13}C cross peak of A2 at 8.37−153.14 ppm in the lower right-hand corner of the HSQC spectrum shown in Figure 4, and the long-range ^{1}H−^{13}C correlation peak between proton A3 and the carbonyl group at 7.77−166.88 ppm shown in Figure 5b served to differentiate protons A2−A3 from A6−A7. The signals at 8.37 and 7.77 ppm were thus assigned to protons A2 and A3, while those at 8.57 and 8.45 ppm were assigned to protons A6 and A7, respectively.

The assignment was carried out further by using ^{1}H−^{13}C correlations. Figure 4 shows the HSQC spectrum of **rac−1a**

(14) Schleucher, J.; Schwendinger, M.; Sattler, M.; Schmidt, P.; Schedletzky, O.; Glaser, S. J.; Sorensen, O. W.; Griesinger, C. *J. Biomol. NMR* **1994**, *4*, 301–306.
(15) Willker, W.; Leibfritz, D.; Kerssebaum, R.; Bermel, W. *Magn. Reson. Chem.* **1993**, *31*, 287–292.

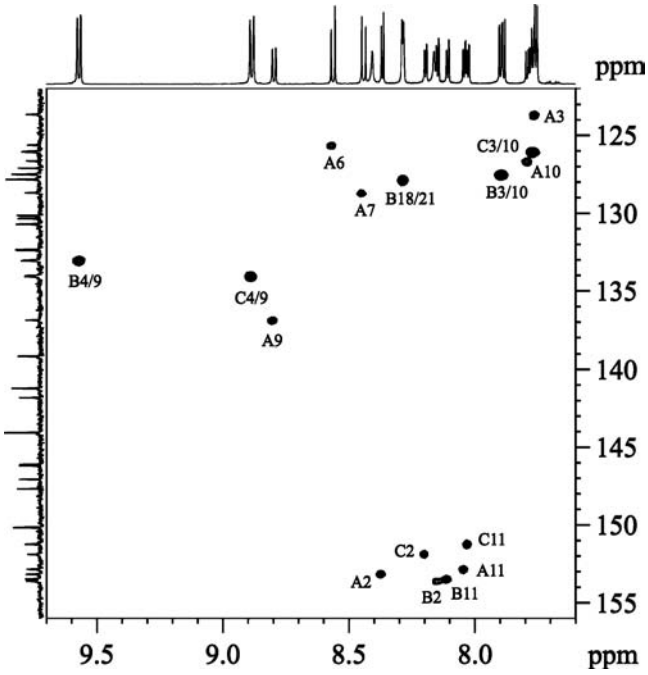

Figure 4. Section of HSQC spectrum of **rac**−**1a** in the aromatic region. The labels are, for assignment, fulfilled by a combined analysis of HMBC and NOESY spectra. See text for more details.

in the aromatic region. In the HSQC spectrum, 16 cross peaks were observed, with five stronger peaks due to the overlapped positions (B4/9, C4/9, B18/21, B3/10, and C3/10). Furthermore, in the lower right-hand corner, six cross peaks were observed. These peaks are due to the CH groups at positions 2 and 11 of the ligands. The differentiation between ligands B and C was fulfilled by considering the long-range $^{1}H-^{13}C$ correlations shown in Figure 5a.

An HMBC spectrum gives us C−H correlation through multiple bonds and is thus versatile in assigning the molecular backbone over quaternary carbons, where neither H−H nor single bond C−H correlations can be observed. Figure 5 shows two sections of the HMBC spectrum of **rac**−**1a**. The correlations between the methyl groups and the quaternary carbons separated by two and three bonds are shown. The ^{13}C signals at 144.04, 130.68/130.70, and 132.31/132.36 ppm were thus assigned to quaternary carbons at positions B19/20, C5/8, and C6/7. Cross peaks between the quaternary carbons at positions C5/8 and protons at 7.77 ppm and between the carbons at C6/7 and the protons at 8.89 ppm were observed (see Supporting Information Figure S1). The ^{1}H signals at 7.77 and 8.89 ppm were thus identified to be due to protons at positions C3/10 and C4/9. This fulfilled the distinction between ligands B and C. In Figure 5b, cross peaks between C═O and protons at 8.42 and 7.77 ppm were observed. The broad peak at 8.42 ppm was thus assigned to be due to one of the protons in the NH_2 group, while the proton at A3 was identified at 7.77 ppm, which overlaps with C3/10. This served to distinguish protons A2−A3 from A6−A7.

By using DQF-COSY and C−H correlations, we have been able to assign signals of ligand A completely. The C_{2v} symmetry in both ligands B and C makes the symmetrical positions chemically equivalent and thus reduces the number

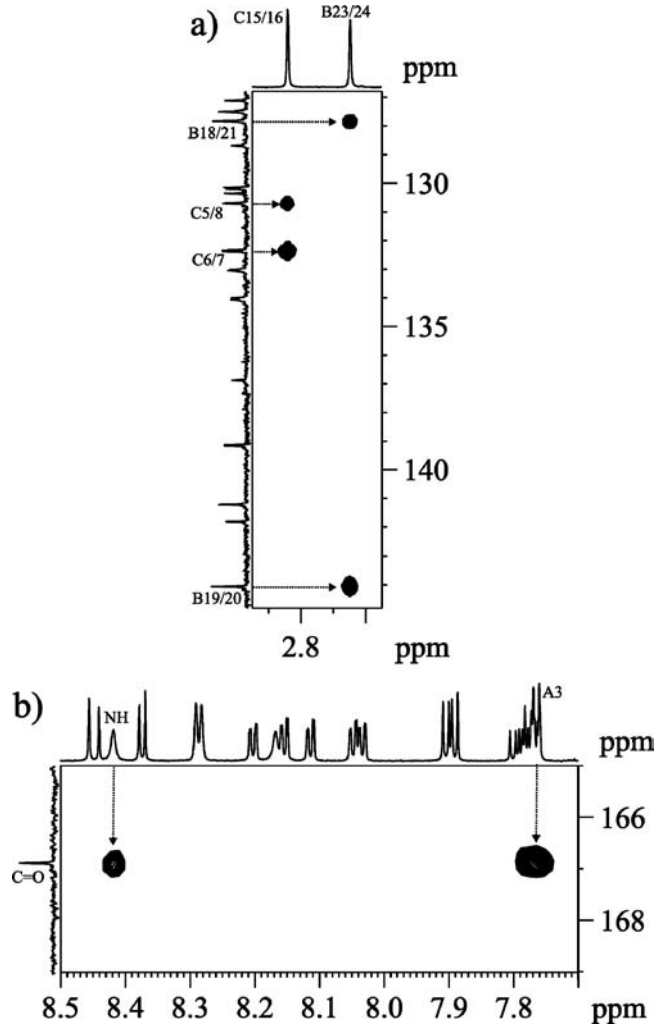

Figure 5. Sections of HMBC spectrum of **rac**−**1a**. (a) Region showing long-range C−H correlation between methyl protons and backbone carbons of ligands B and C, respectively, and (b) region for long-range C−H correlation between C═O and NH and the aromatic proton A3 of ligand A.

of resonance signals by half. Coordination with ruthenium induces a shift in the resonance signals, and we indeed observed coordination-induced shifts on positions 2 and 11. The coordination-induced chemical shifts on the rest of the positions are so weak that the degeneracy in chemical shifts of these positions remains unchanged. Such symmetry makes it difficult for us to distinguish signals of positions 2 and 11 from each other. We were unable to assign positions B2, B11, C2, or C11 using either COSY or C−H correlations. This assignment was fulfilled by observing NOE contacts among the neighboring ligands.

The NOE is based on direct spatial interaction between nuclei; it thus provides us information of distance and spatial arrangement of the molecules. While it plays an important role in the NMR structure of biomacromolecules,[16] it is well-known that NOE is a powerful tool in structural and conformational analysis of small molecules.[17] For example, one of us has successfully applied selective NOEs to determine the stereochemistry of γ-butyrolactones.[18] For

(16) Wüthrich, K. *NMR of Proteins and Nucleic Acids*; Wiley: New York, 1986.

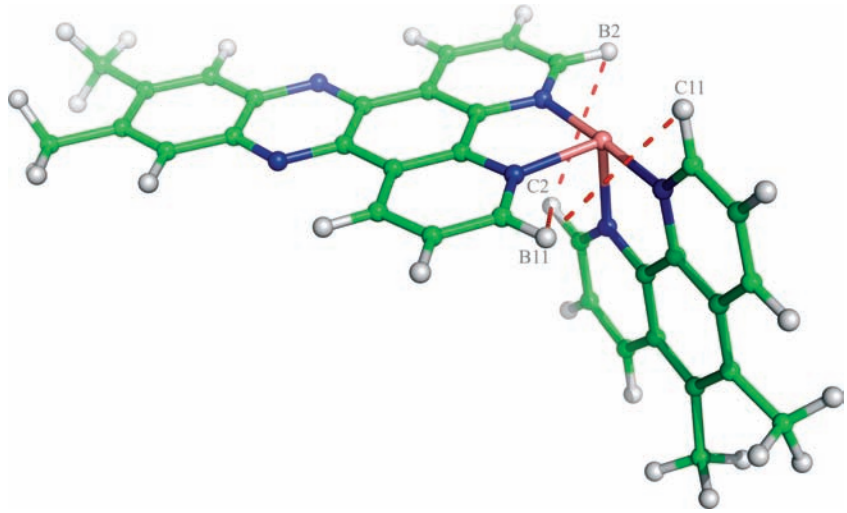

Figure 6. Three dimensional model structure of ruthenium complex, with ligand A omitted for clarity. Atoms showing contacts for NOE observation are highlighted.

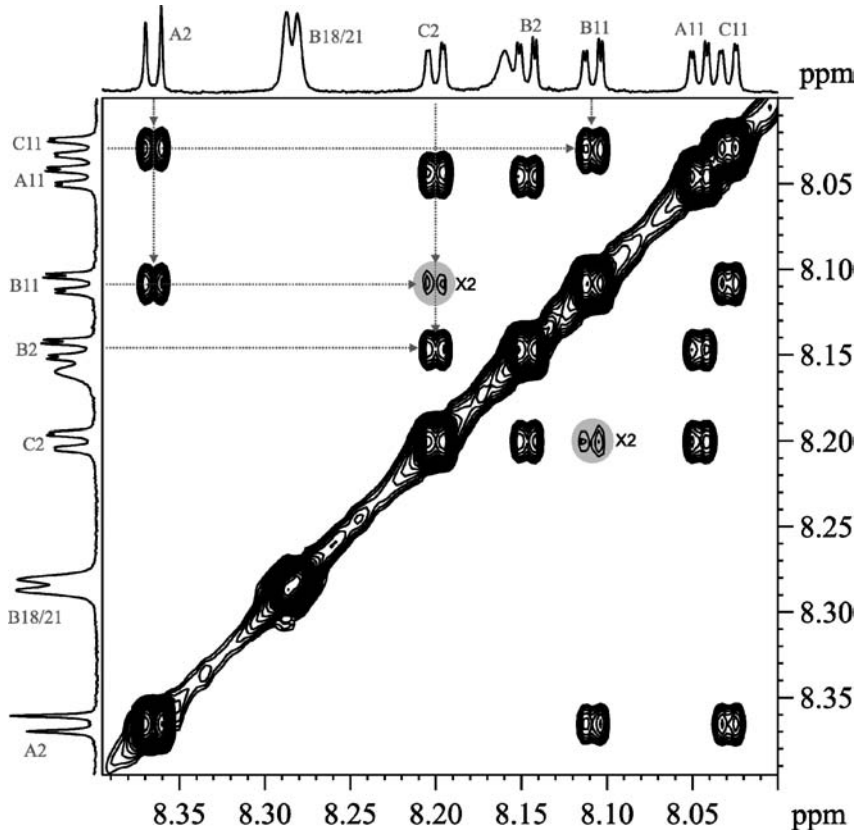

Figure 7. Section of NOESY spectrum of **rac−1a** in the region 8.00−8.40 ppm, where signals of positions 2 and 11 of all the ligands locate. Cross peaks used for the stereo assignment are highlighted. The weak peak B11−C2 is magnified twice.

Table 1. Cross Peaks in NOESY Spectra Showing Inter-Ligand Contact

rac−1a		**rac−1b**	
B2−C2 (s)*	A2−B11 (s)	B2−C2 (s)	A2−B2 (s)
B3−C2 (w)*	A2−C11 (s)	B3−C2 (w)	A2−C2 (s)
B4−C2 (w)	A3−C11 (w)	B4−C2 (w)	A10−C11 (w)
B11−C2 (w)	A11−B2 (s)	B11−C2 (w)	A11−B11 (s)
B11−C11 (s)	A11−C2 (s)	B11−C11 (s)	A11−C11 (s)

* s = strong; w = weak.

studies on the stereochemistry of ruthenium complexes, Kelso et al. used ^{1}H NMR, COSY, and NOE experiments to characterize the diastereoisomers of azobis(2-pyridine)-bridged bis(heteroleptic) diruthenium complexes in the meso and racemic forms.[19] By observing NOE contacts between ligands, Gomez et al. were able to verify the diastereomers of ruthenium bis(bipyridine) complexes containing unsymmetric N,N′ bidentate ligands aryl-pyridine-2-ylmethyl-

(17) Neuhaus, D.; Williamson, M. *The Nuclear Overhauser Effect in Structural and Conformational Analysis*; VCH Publisher: New York, 1989.
(18) Xie, X.; Tschan, S.; Glorius, F. *Magn. Reson. Chem.* **2007**, *45*, 381–388.
(19) Kelso, L. S.; Reitsma, D. A.; Keene, F. R. *Inorg. Chem.* **1996**, *35*, 5144–5153.

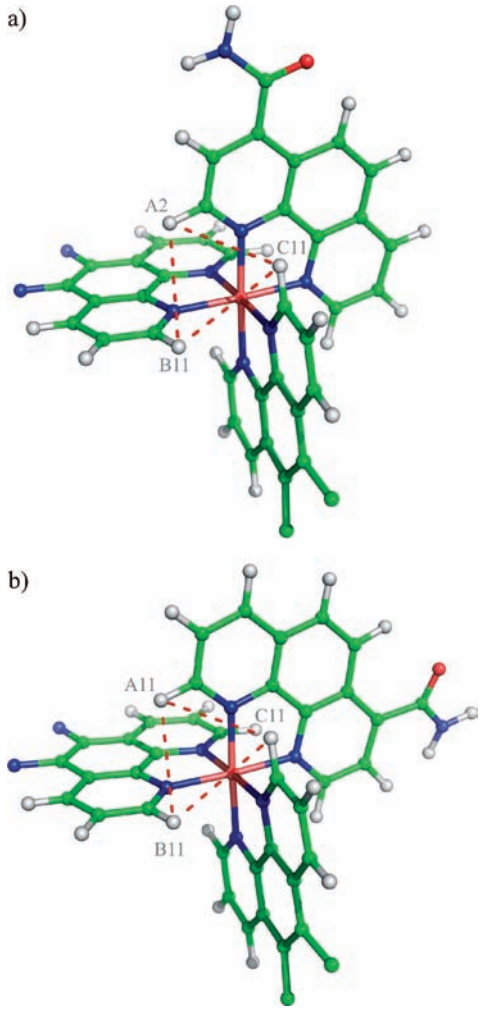

Figure 8. Three dimensional structures of the two diastereomers **Δ−1a** and **Δ−1b**. Atoms showing strong NOE contact characteristic of the corresponding 3D structure are highlighted. Ligands B and C are partially omitted for clarity.

amine.[20] Using mainly the anisotropic shifts in ^{1}H spectra, Hesek et al. determined the major diastereomer of a ruthenium bis(bipyridine) sulfoxide complex as being of the *cis*-Λ- form.[21] Finally, Brunner et al. used ^{1}H anisotropic shifts in combination with X-ray structures to study the stereochemistry of a series of (η^6-arene)ruthenium(II) half-sandwich complexes.[22] In this study, we show for the first time a thorough NOESY study on tris-heteroleptic ruthenium complexes as a method for determining the relative stereochemistry about the metal center. This was fulfilled by using interligand NOEs within the complexes.

Figure 6 shows a three-dimensional model structure of complex **1** with ligands B and C (ligand A is omitted for clarity). The orientation of ligand A results in two distinguishable diastereomers, **rac−1a** and **rac−1b** (see Figure 8). Therefore, the assignment of positions B2/B11 and C2/C11 described here is valid for both diastereomers. The octahedral coordination of the metal center makes position B2 cis to position C2 and trans to position C11, while position B11 is cis to both positions C2 and C11, respectively. Thus, the proton at B2 is in close vicinity to C2 (around 3.5 Å, as predicted by the program CaChe), while B11 is in close vicinity to C11 (around 3.5 Å) and in long-range contact with C2 (around 5.2 Å). By observing the long-range NOE contact between B11 and C2, we were able to differentiate protons B11 from B2, as well as protons C2 from C11. A section of the NOESY spectrum of **rac−1a** containing those cross peaks is presented in Figure 7. Two strong cross peaks at 8.15−8.20 ppm and 8.11−8.03 ppm and a weak one at 8.11−8.20 ppm were observed. The two strong cross peaks are caused by protons close to each other, whereas the weak one is due to a long-range contact. The signals at 8.15 and 8.11 ppm are due to ligand B, while those at 8.20 and 8.03 ppm are of ligand C. The signals at 8.11 and 8.20 ppm responsible for a long-range NOE contact were thus assigned to protons B11 and C2, respectively. This led to the assignment of the peaks at 8.15 and 8.03 ppm to protons B2 and C11, respectively. Thus, with this final signal assignment at positions 2 and 11, we have succeeded in a full characterization of all the ligands. The assigned chemical shifts of **rac−1a** are listed in Table S1 (see the Supporting Information).

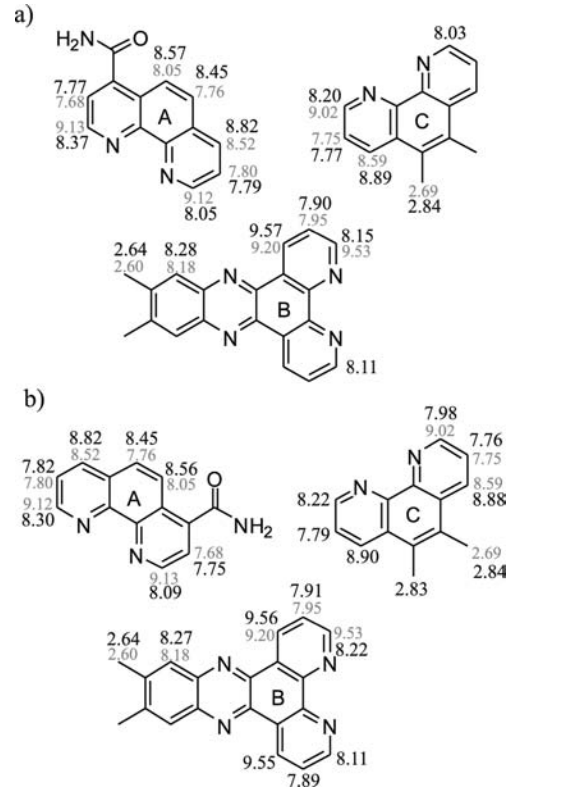

Figure 9. ^{1}H chemical shifts of free ligands (gray) and **rac−1a** (a) and **rac−1b** (b) in DMSO-d_6. Identical values of the corresponding equivalent positions are omitted for clarity.

Assignment of Relative Configurations. Because of the lower symmetry of ligand A, its coordination with the metal center results in two diastereomers, whose 3D model structure is presented in Figure 8. As highlighted in Figure

(20) Gomez, J.; Garcia-Herbosa, G.; Cuevas, J. V.; Arnaiz, A.; Carbayo, A.; Munoz, A.; Falvello, L.; Fanwick, P. E. *Inorg. Chem.* **2006**, *45*, 2483–2493.
(21) Hesek, D.; Inoue, Y.; Everitt, S. R.; Ishida, H.; Kunieda, M.; Drew, M. G. B. *Inorg. Chem.* **2000**, *39*, 317–324.
(22) Brunner, H.; Zwack, T.; Zabel, M. *Organometallics* **2003**, *22*, 1741–1750.

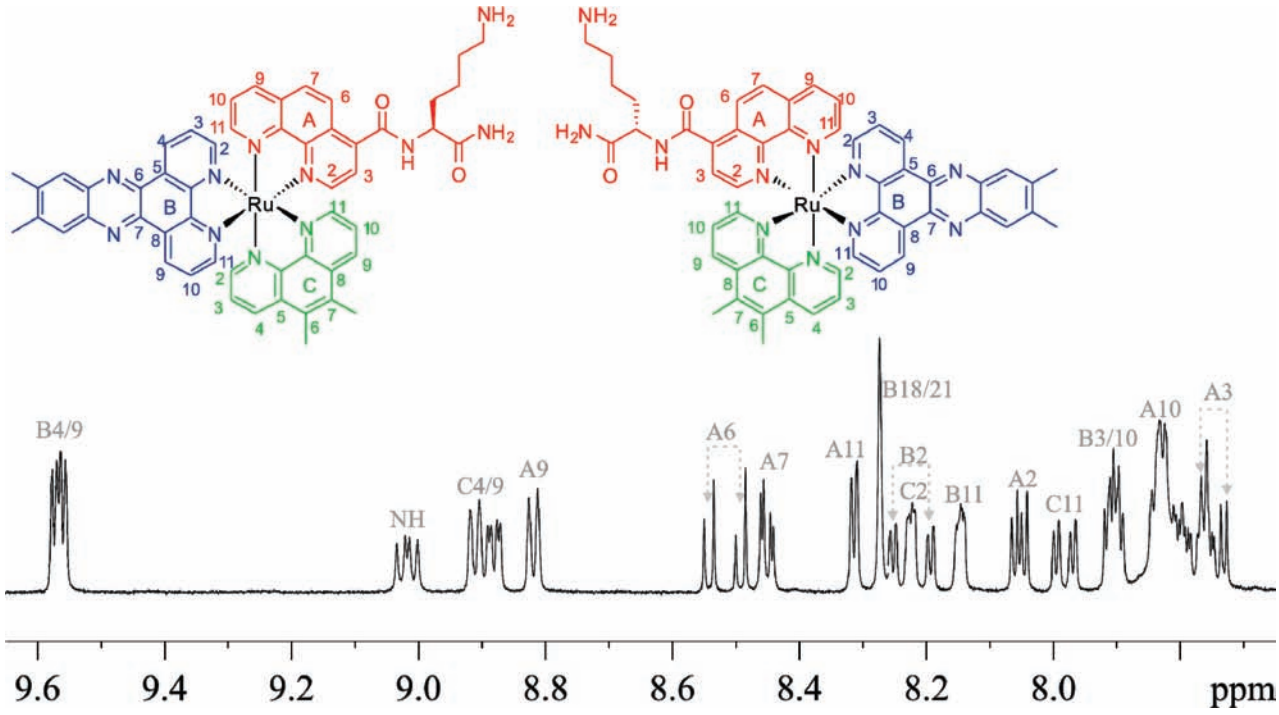

Figure 10. Aromatic region of the ^{1}H spectrum of **Δ−2b** and **Λ−2b**. The corresponding chemical structures are also provided. The labels are for assignment.

8, position A2 is cis to both B11 and C11 in **rac−1a**, whereas position A11 takes the corresponding place in **rac−1b**. The distance between these positions predicted by the program CaChe (Fujitsu) is about 3.5 Å; therefore, we would expect characteristic NOESY cross peaks for **rac−1a** between A2−B11 and A2−C11 and between A11−B11 and A11−C11 for **rac−1b**. Indeed, Table 1 shows these observed cross peaks, thus enabling us to complete a full assignment of the resonance signals and allowing us to confirm the relative stereochemistry of **rac−1a** and **rac−1b**. The assigned chemical shifts of **rac−1b** are listed in Table S2 (see the Supporting Information).

Coordination Induced Shifts (CIS) and Coordination Properties of the dppz and phen Ligands. In order to take a closer look into the coordination properties of the different bidentate ligands for ruthenium complexation, we took ^{1}H spectra of all of the free ligands in the same solvent and analyzed their CIS. The chemical shifts of the ligands in free form and after coordination with ruthenium in **rac−1a** and **rac−1b** are shown in Figure 9. Inspection of Figure 9a reveals that the degeneracy in chemical shifts due to the C_{2v} symmetry of ligand B (dppz) remains unchanged in **rac−1a** (except for a 0.04 ppm difference between positions 2 and 11), which suggests a very similar anisotropic effect of the substituted phenanthrolines in this arrangement. Similar results were observed by Myari et al.[23] in the bis-heteroleptic complex attached with a short amino acid sequence [Ru(bpy)$_2$(m-bpy-GHK)]Cl$_2$ (GHK = glycine-L-histidine-L-lysine, m-bpy = 4-methyl-2,2′-bipyridine), where the degeneracy in ^{1}H chemical shifts of the two bpy ligands was detected. The CIS of dppz is 1.38 and 1.42 ppm at positions 2 and 11, respectively, while it is 0.82 and 0.99 ppm for Me$_2$phen at 2 and 11 and 0.76 and 1.07 ppm for A2 and A11, respectively. The coordination-induced shift in the ligand dppz is larger than that in the phenanthroline derivatives, which indicates the former to be a stronger σ donor and π acceptor.[7] Inspection of Figure 9b reveals the removal of the degeneracy in dppz of **rac−1b**: position 2 has a 0.07 downfield shift, while position 11 remains unchanged as compared with the corresponding position in **rac−1a**. This can be understood by looking into the orientation of ligand A in **rac−1b**. The ligands are arranged in such a way that one-half of the dppz (containing position 2) is located in the region of the anisotropic ring current effect of the 4-carboxamide-substituted pyridine ring of A, whereas another half (containing position 11) confronts the anisotropic effect of a nonsubstituted pyridine ring of C in a similar way as in **rac−1a**. Thus, for the ligands possessing C_{2v} symmetry, the observed different chemical shifts of positions 2 and 11 are caused by the different anisotropic effect of the neighboring ligands.[9] Inspection of ligand C (Me$_2$Phen) reveals a weaker upfield shift in position 2 than in position 11. Since positions C2 and C11 are located in the anisotropic region of dppz and substituted phen, respectively, we may thus deduce that the ligand dppz causes a somewhat weaker anisotropic effect than a phen ligand does. Since dppz has a larger π network, the electron density is likely more delocalized, which results in a weaker ring current and thus a weaker anisotropic effect. It was indirectly evidenced by Freedman et al. that the phen ligand induces a greater upfield shift than a bpy-type ligand,[9] while comparison between the ligands dppz and phen has never been published previously. Although [Ru(phen)$_2$-dppz]$^{2+}$ complexes were found to show binding activity with

(23) Myari, A.; Hadjiliadis, N.; Garoufis, A. *Eur. J. Inorg. Chem.* **2004**, *142*, 7–1439.

DNA,[24] no detailed NMR spectroscopic characterization of the metal complexes was ever published. We present for the first time a thorough characterization of the tris-heteroleptic Ru(II) complexes and give a comparison of the coordination properties of the phen and dppz ligands.

As an additional experiment, we thought that the introduction of an additional chiral center would destroy enantiomerism and allow us to observe two sets of peaks for each relative diastereomer. We thus synthesized complex **2** (Figure 1), which contains carbon-centered chirality in ligand A in addition to the metal-centered chirality. This results in the degenerate pairs of enantiomers from **1** becoming distinct diastereomers themselves when L-lysine is attached. That is, each diastereomer contains two stereoisomers, combining to give four species overall, **Δ−2a**, **Λ−2a**, **Δ−2b**, and **Λ−2b**. We were able to separate the relative diastereomers **Δ−2a** and **Λ−2a** from **Δ−2b** and **Λ−2b**, and shown in Figure 10 is the ^{1}H spectrum of **Δ−2b** and **Λ−2b** in the aromatic region. Two sets of signals with very similar chemical shifts were observed at positions A2, A3, A6, A7, and A10 for ligand A; B2, B3/10, B4/9, and B11 for ligand B; and C2, C3/10, C4/9, and C11 for ligand C. With a careful analysis of their H−H and C−H correlation spectra, we were able to assign all of the signals. A full list of chemical shifts is provided in the Supporting Information. The assignment of relative stereochemistry was performed in a similar manner to that for complex **1** by examining interligand cross peaks in NOESY spectra (see Supporting Information Figure S2). Strong cross peaks A2−B2, A2−C2, A11−B11, and A11−C11 were observed for **Δ−2b** and **Λ−2b** and their stereo-structures verified.

(24) Dupureur, C. M.; Barton, J. K. *Inorg. Chem.* **1997**, *36*, 33–43.

Conclusion

In summary, we used two-dimensional NMR experiments, DQF-COSY, HSQC, and HMBC to assign both ^{1}H and ^{13}C signals of tris-heteroleptic ruthenium (II) polypyridyl complexes [Ru(pp)(pp′)(pp″)](PF$_6$)$_2$. Further analysis of NOE contacts between ligands allowed us to make a full signal assignment for these types of complexes for the first time and to determine the relative stereochemistry. Thus, this strategy provides a quick and reliable method for the stereochemical assignment of tris-heteroleptic ruthenium(II) complexes when other methods are inferior. Further, a comparison of the coordination properties between the phen and dppz ligands provides us with useful information for designing ruthenium complexes where electrochemical and steric properties are concerned.

Acknowledgment. We gratefully acknowledge the Deutsche Forschungsgemeinschaft for funding the Bruker AVANCE 600 spectrometer. S.P.M. thanks the NIH for a Chemistry−Biology Interface Training Grant Fellowship (T32 GM 071339). E.M. also acknowledges support from NIH (GM 071695).

Note Added after ASAP Publication. Due to production errors, this article was published ASAP on December 23, 2008, with Figures 2−7 identified incorrectly. The corrected article was published ASAP on January 8, 2009.

Supporting Information Available: Lists of ^{1}H and ^{13}C chemical shifts and a HMBC spectrum of **rac−1a**. This material is available free of charge via the Internet at http://pubs.acs.org.

IC801744A